Review



# Superconductors Exhibiting Enhanced or Diminished Resonance Characteristics within the Framework of the Bardeen-Cooper-Schrieffer Model

Je Huan Koo *

Posted Date: 2 January 2024

doi: 10.20944/preprints202312.2308.v1

Keywords: Superconductors; Cuprates; Pnictides

*Review*

# Superconductors Exhibiting Enhanced or Diminished Resonance Characteristics within the Framework of the Bardeen-Cooper-Schrieffer Model

**Je Huan Koo**

Department of Electrical and Biological Physics, Kwangwoon University, Seoul 01897, Republic of Korea; djhkoo@gmail.com/koo@kw.ac.kr; Tel:+82-(0)2-940-8257, Fax:+82-(0)2-6442-2269

**Abstract:** The elevated or depressed transition temperatures observed in cuprate and pnictide superconductors and other exotic superconductors pose a challenge in the context of explaining them through the traditional Bardeen-Cooper-Schrieffer (BCS) models of superconductivity. A significant obstacle in understanding this phenomenon can be addressed by considering an alternative electron distribution. Our investigation has identified an anyonic distribution, where the occupancy of a site created by removing a hole is filled by an electron. In heavy fermion superconductors (HFSs) block spins must be included in the distribution. The interplay, that is, resonance between superconducting electrons within the conventional BCS framework and independent charge density waves (CDWs) might contribute to driving the high-transition-temperature superconductors (HTSCs).

**Keywords:** Superconductors; Cuprates; Pnictides

**PACS:74.72.Mn;** 75.30.Fv; 72.15.Nj

## 1. Introduction

The conductive characteristics of low-temperature superconductors, as documented by Onnes [1], can be effectively elucidated through the Bardeen-Cooper-Schrieffer (BCS) theory [2]. In 1986, Bednorz and Müller [3] explored copper oxide compounds in quasi-two-dimensional (2D) electronic structures, unveiling the existence of high-temperature superconductors. Nevertheless, comprehending the electrical resistivity at temperature, the remarkably high superconducting transition temperature, and the dependence on the origin of the pseudogap necessitates a lucid explanation for achieving precise alignment among theoretical frameworks for high-transition-temperature superconductors (HTSCs). Numerous models have been posited to expound the HTSC phenomenon, including the s = 3/2 hole composite model [4,5], ferromagnetic cluster theory [6,7], spin fluctuation [8–10], and resonating valence bonds (RVBs) [11–13]. A theoretical framework for HTSC is currently under development, employing both the Heisenberg antiferromagnetic model with Green's function form [14] and the attractive Hubbard model with mean-field theory [15]. Cuprate superconductors manifest 2D superconductivity in the $CuO_2$ plane, while Fe-As compounds exhibit two-dimensional superconductivity in the Fe-As plane. Hence, the lower dimensions of these systems are intricately linked to superconductivity. The elevated transition temperatures of HTSCs surpass those of traditional BCS superconductors, indicating an alternate mechanism or a considerably more intricate BCS-type mechanism. As an alternative proposition, a different electron distribution, rather than the Fermi-Dirac distribution, can be applied to heavy fermion superconductors [16] within pure BCS frameworks. This paper delineates such an electron distribution applicable to HTSCs.

## 2. Theory

Preprints (www.preprints.org) | NOT PEER-REVIEWED | Posted: 2 January 2024 doi:10.20944/preprints202312.2308.v1



Let's begin by examining high-temperature superconductors (HTSCs) that share similarities with BCS superconductors. The Hamiltonian for low-transition-temperature superconductors, following the BCS type [2], is expressed as:

$$H_{BCS} = \sum_{k,\sigma} (\varepsilon_{k,\sigma}) a^{+}_{k,\sigma} a_{k,\sigma} + \sum_{k,k',q,\sigma,\sigma'} \frac{1}{2} (U_{BCS} + U_c) a^{+}_{k+q,\sigma} a^{+}_{k'-q,\sigma'} a_{k',\sigma'} a_{k,\sigma} \quad (1)$$

where the BCS-type electron-electron interaction [1] is given by:

$$U_{BCS} = \frac{2g^2 \hbar\omega_q}{(\varepsilon_{k+q,\sigma} - \varepsilon_{k,\sigma'})^2 - (\hbar\omega_q)^2} \quad (2)$$

In these equations, $\hbar\omega_q$ is the phonon energy, $g$ is the coupling constant of electron-phonon interactions, $\sigma$ designates the spin states, $\varepsilon_{k,\sigma}$ is the electron kinetic energy, $a_{k,\sigma}$ is an annihilation operator, and $U_c$ is the Coulomb interaction.

When used with the BCS approach, the reduced BCS-type Hamiltonian thus becomes:

$$\begin{aligned} H_{BCS} &= \sum_{k,\sigma} (\varepsilon_{k,\sigma}) a^{+}_{k,\sigma} a_{k,\sigma} - \sum_{k,k',q,\sigma,\sigma'} (\Delta_k a^{+}_{k\uparrow} a^{+}_{-k\downarrow} + \Delta^{*}_k a_{-k\downarrow} a_{k\uparrow} - \Delta_k b^{*}_k) \\ \Delta_k &= -\sum_{k'} V_{kk'} b_{k'}, V_{kk'} = U_{BCS} + U_c \\ b_k &= < a_{-k\downarrow} a_{k\uparrow} > \end{aligned} \quad (3)$$

The brackets <> denote the average of the mean field, and $\Delta_k$ is the superconducting gap.

Using the Bogoliubov transformation [17], the operators are given by:

$$\begin{aligned} a_{k\uparrow} &= u^{*}_k \gamma_{k0} + v_k \gamma^{+}_{k1} \\ a^{+}_{-k\downarrow} &= -v^{*}_k \gamma_{k0} + u_k \gamma^{+}_{k1} \end{aligned} \quad (4)$$

Here, the operator $\gamma_{k0}$ corresponds to a quasiparticle composed of an electron $(k\uparrow)$ with amplitude $u_k$ and a hole $(-k\downarrow)$ with amplitude $v_k$.

Let's explore anyonic distributions in the scenario where electrons inhabit a site with removed holes and anyonic states, depicted in Figure 1. A novel anyonic distribution, termed the Kwangwoon distribution, can be deduced:

$$\begin{aligned} f_{anyon} &= f^{FD}_{hole} - f^{FD}_{electron} \equiv \tanh \frac{\varepsilon - \mu}{2k_B T} = f_{anyon} \\ f^{FD}_{hole} &= \frac{1}{1 + \exp(-\frac{\varepsilon - \mu}{k_B T})} \\ f^{FD}_{electron} &= \frac{1}{1 + \exp(\frac{\varepsilon - \mu}{k_B T})} \end{aligned} \quad (5)$$

Preprints (www.preprints.org) | NOT PEER-REVIEWED | Posted: 2 January 2024 doi:10.20944/preprints202312.2308.v1



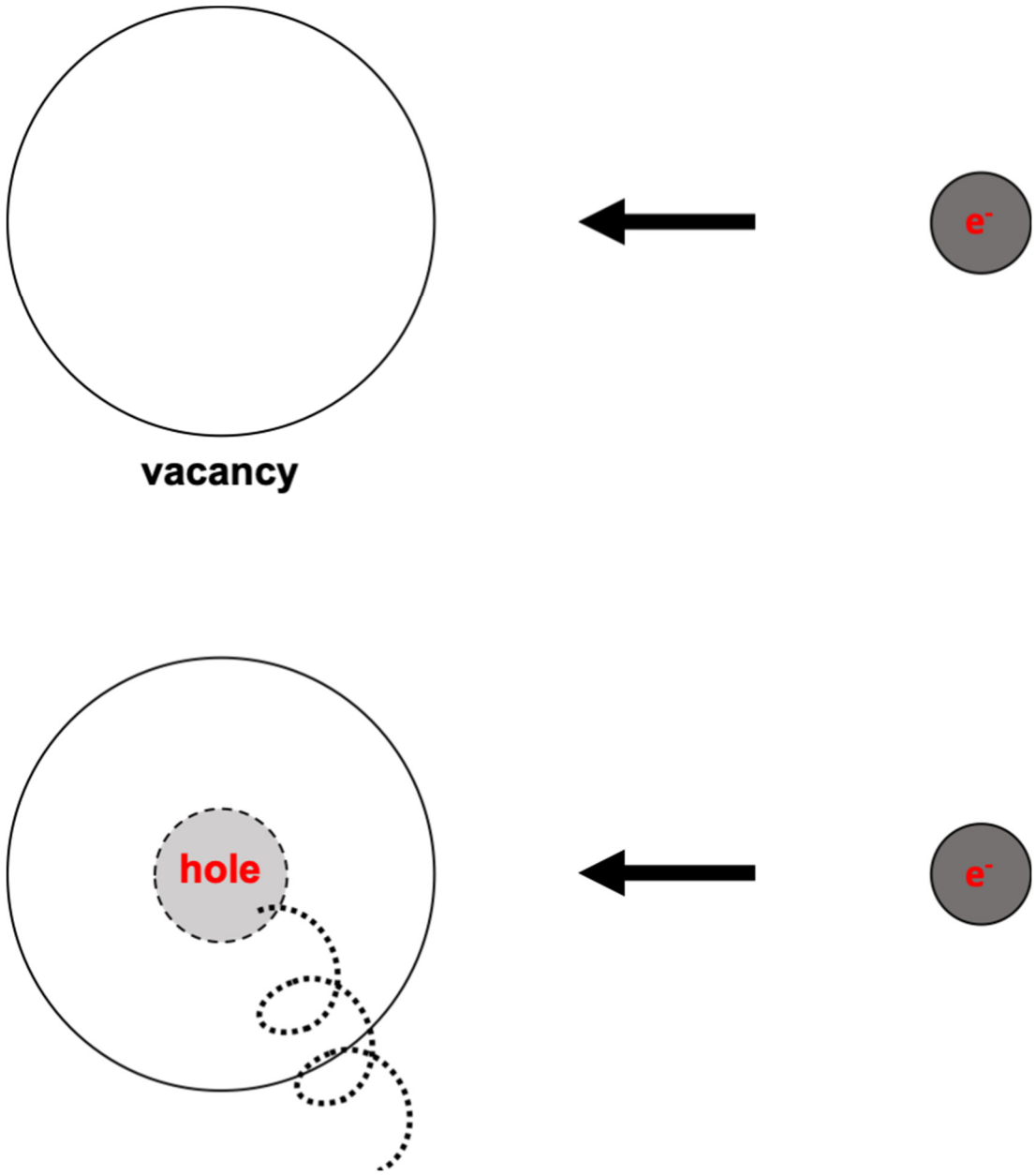


**Figure 1.** Electrons occupying the site of deleted holes or the site of a vacancy are differentiated.

Here, $\varepsilon$ is the energy, $\mu$ is the chemical potential, $k_B$ is the Boltzmann constant, $T$ is the temperature, and FD means Fermi-Dirac distribution (Figure 1). A new distribution can be justified as follows. Figure 1 shows two cases as two different operators, including creation and annihilation, and a vacuum is denoted by |0>. Occupation is $a^{+}a\,|\,0>, \tilde{a}^{+}a\,|\,0>$. $\tilde{a}^{+}$ is a creation operator of an electron, $a$ is an annihilation operator of a hole, and anyonic states denote $\tilde{a}^{+}a$. $k_B$ is Boltzmann's constant, $\mu$ is the chemical potential, $\varepsilon_l$ is the energy, and $T$ is the temperature.

Preprints (www.preprints.org) | NOT PEER-REVIEWED | Posted: 2 January 2024 doi:10.20944/preprints202312.2308.v1



We may regard electrons and holes as different electrons from two dissimilar bands in which the distribution is $\tanh(\frac{\varepsilon_k-\mu}{2k_BT})$, which originates from the grand partition function of

$$Z=\Pi_{k=1}^{\infty}\sum_{n_k=0}^{1}e^{-\beta(\varepsilon_k-\mu)^{n_k}}\sum_{n_k^{'}=0}^{1}e^{\beta(\varepsilon_k-\mu)^{n_k^{'}}}$$

$$\beta=1/(k_BT),\frac{\partial}{\partial\{\beta(\varepsilon_k-\mu)\}}\ln Z=distribution$$

The HTSC gap equation is given by:

$$\Delta_k=-\sum_{k'}V_{kk'}\Delta_{k'}[1-2f(E_{k'})]/2E_{k'}$$

$$f(E_{k'})=1/[1+\exp(E_{k'}/k_BT)]\Rightarrow\tanh(E_{k'}/(2k_BT))\ (6)$$

$$E_{k'}=\sqrt{(\varepsilon_{k'})^2+(\Delta_{k'})^2}$$

where the distribution may be changed.

Using similar methods [17] and these equations for HTSCs, the resulting superconducting gap is given by:

$$1=NV\int_0^{\hbar\omega}\frac{d\varepsilon[2\tanh\{\sqrt{\varepsilon^2+(\Delta)^2}/(2k_BT)\}-1]}{\sqrt{\varepsilon^2+(\Delta)^2}}$$

$$N(0)|U_{BCS}+U_c|=NV \qquad (7)$$

$$-1+2NV\ln\frac{1.14\hbar\omega}{k_BT}-NV\sinh^{-1}\frac{\hbar\omega}{\Delta}-2NV\frac{\Delta^2}{\pi^2(k_BT)^2}\frac{7}{8}(1.2)=0$$

Here, the constants are obtained from a previous study [17], $\hbar\omega$ is the phonon energy, and $N(0)$ is the density of the states at the Fermi level.

Let us now consider the spin relaxation rate in the superconductors.

From Hebel and Slichter [17], this is given as:

$$R=1/T_1$$

$$R_s/R_n=2\int_0^{\infty}[\rho_s^{'}(x,\eta,\delta)]^2(1+\frac{\eta}{x^2})f(x)(1-f(x))dx$$

$$x=E/k_BT,\delta=\delta E/k_BT,\eta=\Delta/k_BT$$

These parameters are described in detail in [17], and s and n indicate superconducting and normal, respectively. In the case of a Fermi-Dirac distribution, f(x), this has a peak below the transition temperatures. However, this might have no peak in the case of an anyonic distribution, as $f(x)=\tanh\frac{x}{2}$, which is in line with the HTSC experiments.

Let us next consider the superconducting coherence length in HTSCs. We can regard the coherence length as the diameter in an orbital so that from Bohr's conjecture, $\xi=2r,2\pi r=n\lambda,\lambda=\frac{h}{mv}$, and $n$ is an integer. $h$ is the Planck constant, $m$ is the mass of the electron, and $v$ is the velocity of an electron. This becomes:

Preprints (www.preprints.org) | NOT PEER-REVIEWED | Posted: 2 January 2024 doi:10.20944/preprints202312.2308.v1



$$1 = NV\int_0^{\hbar\omega} \frac{d\varepsilon[2\tanh\{\sqrt{\varepsilon^2+(\Delta)^2}\,/(2k_BT)\}-1]}{\sqrt{\varepsilon^2+(\Delta)^2}}$$

$$v = v_F\int_0^{\hbar\omega} \frac{d\varepsilon[2\tanh\{\sqrt{\varepsilon^2+(\Delta)^2}\,/(2k_BT)\}-1]}{\sqrt{\varepsilon^2+(\Delta)^2}}$$

$$N(0)\,|\,U_{BCS}+U_c\,|=NV$$

$$-1+2NV\ln\frac{1.14\hbar\omega}{k_BT}-NV\sinh^{-1}\frac{\hbar\omega}{\Delta}-2NV\frac{\Delta^2}{\pi^2(k_BT)^2}\frac{7}{8}(1.2)=0 \qquad (8)$$

$$\therefore\quad \xi = 2r = \frac{h}{\pi mv} = \frac{h}{\pi mv_F}NV$$

where $v_F$ is the Fermi velocity.

We next consider spin gaps and pseudogaps in HTSC. These can be approximated by:

$$\tanh(x) \approx x-\frac{1}{3}x^3 \quad for\ x\approx 0$$
$$\approx 1-2e^{-2x} \quad for\ x>>1, \qquad (9)$$

At the high-temperature limit and low-temperature limit, the difference of two limits for the distribution of Eq. (5) can be transformed as the spin gap as:

$$\Delta_{spin-gap} = \int_0^{\hbar\omega}[\frac{\varepsilon}{2k_BT}-\frac{1}{3}(\frac{\varepsilon}{2k_BT})^3-\{1-2e^{-\frac{2\varepsilon}{2k_BT}}\}]d\varepsilon$$
$$=\frac{(\hbar\omega)^2}{4k_BT}-\frac{1}{96}\frac{(\hbar\omega)^4}{(k_BT)^3}-\hbar\omega-2k_BT(e^{-\frac{2\hbar\omega}{2k_BT}}-1) \qquad (10)$$

where $\hbar\omega$ is the Debye cutoff energy, as shown in Figure 2. Pseudogaps are given as:

$$-1 = N\tilde{V}\int_0^{\hbar\omega} \frac{d\varepsilon[2\tanh\{\sqrt{\varepsilon^2+(\Delta_{PG})^2}\,/(2k_BT)\}-1]}{\sqrt{\varepsilon^2+(\Delta_{PG})^2}}$$

$$\Delta_{PG} = \Delta_{pseudo-gap}$$

$$+1+2N\tilde{V}\ln\frac{1.14\hbar\omega}{k_BT}-N\tilde{V}\sinh^{-1}\frac{\hbar\omega}{\Delta_{PG}}-2N\tilde{V}\frac{\Delta_{PG}^2}{\pi^2(k_BT)^2}\frac{7}{8}(1.2)=0$$

$$N(0)(U_{BCS}+U_c)\equiv N\tilde{V} \qquad .(11)$$

$$2\tanh\{\sqrt{\varepsilon^2+(\Delta_{PG})^2}\,/(2k_BT)\}-1<0\,,U_{BCS}+U_c>0\ for\ T_c\le T\le T_{PG}$$

$$2\tanh\{\sqrt{\varepsilon^2+(\Delta)^2}\,/(2k_BT)\}-1>0,U_{BCS}+U_c<0\ \ for\ 0\le T\le T_c$$

$T_c$ : superconducting transition temperature

$T_{PG}$ : on-set temperature of pseudo-gap

Preprints (www.preprints.org) | NOT PEER-REVIEWED | Posted: 2 January 2024 doi:10.20944/preprints202312.2308.v1



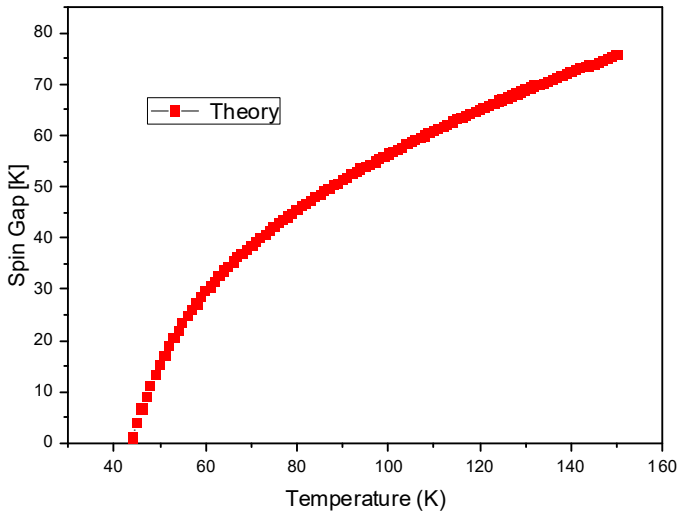


**Figure 2.** A spin gap where the Debye cutoff is 150 K.

Let us then consider the linear resistivity via resonance given as:

$$\text{resonance energy} \Leftrightarrow eE_0 d = eV_0$$

$$resonance \Leftrightarrow \delta(E - E_0)$$

$$J_{current\ density} = \tilde{J} = nev \times \tanh \frac{\varepsilon_F \pm eEd - \mu}{2k_B T} = \sigma E$$

$$\rho = 1/\sigma = 1/[\frac{\partial \tilde{J}}{\partial E}] = \pm 2k_B T \frac{1}{neved} \frac{1}{\tanh^2(\frac{\varepsilon_F \pm eEd - \mu}{2k_B T}) - 1}$$

$$resonance \Rightarrow \rho^{eff} = \int \rho \delta(E - E_0) d(E/E_0) \Leftrightarrow \varepsilon_F \pm eE_0 d - \mu = 0$$

$$\rho^{eff} = \pm 2k_B T \frac{1}{neved} \frac{1}{\tanh^2(\frac{\varepsilon_F \pm eE_0 d - \mu}{2k_B T}) - 1} = 2k_B T \frac{1}{neved} \propto T \quad for\ T \to \infty$$

$$\rho \propto T \quad for\ T \to \infty \qquad . (12)$$

$$\rho_{HTSC} \sim T^5(electron) - T^5(hole) \Rightarrow 0$$

$$\rho : resistivity$$

$$\sigma : conductivity$$

$$V = Ed : voltage$$

$$E : electric\ field$$

$$\mu : chemical\ potential$$

Here, $\rho^{eff}$ is an effective resistivity, $\delta$ means a delta function, $n$ denotes the number density, $v$ signifies velocity, and resistivity $T^5$ is nullified by the presence of electrons and holes. Under optimal doping conditions, an observed quadratic-temperature dependence is attributed not to electron-electron interaction but rather to electron-hole cancellation, resulting in a resistivity derivative with a dependence on temperature squared, as elucidated by:

Preprints (www.preprints.org) | NOT PEER-REVIEWED | Posted: 2 January 2024 doi:10.20944/preprints202312.2308.v1



$$\tilde{\rho} = 1/\tilde{\sigma} = 1/[\frac{\partial^2 \tilde{J}}{\partial E^2} E] \sim T^2 \cdot$$

**3. Discussion**

In the case of direct current, if $\phi_1$ is the probability amplitude of electrons in the conduction band on one side of a junction (the work function), and $\phi_2$ is the amplitude on the field-emitted electron band located outside the surface of the material, the time-dependent Schrödinger equation, $i\hbar\frac{\partial \phi}{\partial t} = \mathcal{K}\phi$, is applied, giving

$$i\hbar\frac{\partial \phi_1}{\partial t} = \hbar\tilde{T}\phi_2 \; ; \; i\hbar\frac{\partial \phi_2}{\partial t} = \hbar\tilde{T}\phi_1 \tag{13}$$

Here, $\hbar\tilde{T}$ represents the effects of transfer interactions across the work function along the axis of energy. In this case, $\hbar\tilde{T} = eV - \varphi$, where $V$ is the external voltage (= electric potential difference), $\varphi$ is the work function, and $t$ is the specific time. We then have

$$\frac{\partial}{\partial t}(\phi_1 + \phi_2) = -i\tilde{T}(\phi_1 + \phi_2) \; ; \; \frac{\partial}{\partial t}(\phi_1 - \phi_2) = i\tilde{T}(\phi_1 - \phi_2) \quad . \tag{14}$$

The amplitudes are

$$\begin{aligned} \phi_1 &= \sqrt{n_1}(e^{i\tilde{T}t} + \alpha e^{-i\tilde{T}t}) \\ \phi_2 &= \sqrt{n_2}(e^{i\tilde{T}t} - \alpha e^{-i\tilde{T}t}) \quad , \\ 1 &= 1 + \alpha^2 \pm 2\alpha\cos(2\tilde{T}t) \end{aligned} \tag{15}$$

where $n_i$ is the number electron densities, $n_1 \approx n_2, \frac{\partial n_1}{\partial t} = -\frac{\partial n_2}{\partial t}$, and $\alpha$ is a normalized factor.

From the relationship given as

$$J \propto \frac{\partial}{\partial t}[\frac{\phi_1^* \phi_2 + \phi_1 \phi_2^*}{\phi_1^2 + \phi_2^2}] = \frac{\mathrm{Re}\{\frac{\partial}{\partial t}\phi_1\}}{\mathrm{Re}\{\phi_2\}} \quad , \tag{16}$$

the resultant pseudo-Josephson direct current is

$$J = J_0 \tan \tilde{T}t \quad , \tag{17}$$

where * indicates the Hermitian conjugate, and Re denotes the real part.

The pseudo-Josephson effect on alternating current is given by

$$i\hbar\frac{\partial \phi_1}{\partial t} = \hbar\tilde{T}\phi_2 - eV\phi_1 \; ; \; i\hbar\frac{\partial \phi_2}{\partial t} = \hbar\tilde{T}\phi_1 + eV\phi_2 \quad , \tag{18}$$

where $eV$ is the electric potential energy. In this case, the amplitudes are

$$\begin{aligned} \phi_1 &= \sqrt{n_1}(e^{i\tilde{T}t} + \alpha_1 e^{-i(\tilde{T}t - eVt)}) \\ \phi_2 &= \sqrt{n_2}(e^{i\tilde{T}t} - \alpha_1 e^{-i(\tilde{T}t - eVt)}) \quad , \\ 1 &= 1 + \alpha_1^{\,2} \pm 2\alpha_1\cos(2\tilde{T}t - eVt) \end{aligned} \tag{19}$$

where $n_i$ is the number electron densities, $n_1 \approx n_2, \frac{\partial n_1}{\partial t} = -\frac{\partial n_2}{\partial t}$, and $\alpha_1$ is a normalized factor.

The resultant pseudo-Josephson for alternating current is

Preprints (www.preprints.org) | NOT PEER-REVIEWED | Posted: 2 January 2024 doi:10.20944/preprints202312.2308.v1



$$J = J_0 \frac{\sin\tilde{T}t + \alpha_1(1-\frac{eV}{\tilde{T}})\sin(\tilde{T}t - eVt)}{\cos\tilde{T}t + \alpha_1\cos(\tilde{T}t - eVt)} \quad . \qquad (20)$$
$$= J_0 \frac{\sin\tilde{T}t \pm 2\cos(2\tilde{T}t - eVt)(1-\frac{eV}{\tilde{T}})\sin(\tilde{T}t - eVt)}{\cos\tilde{T}t \pm 2\cos(2\tilde{T}t - eVt)\cos(\tilde{T}t - eVt)} \quad .$$

Let us consider perturbation theory using the Josephson formalism along the axis of energy. For potentials as a junction, $(\text{Potentials}: V_0, V_1\ (V_0 >> V_1) \Leftrightarrow \text{Josephson junction}\ V_0 : V_1 : V_0)$, the energies for $V_0$ and $V_1$ are

$$\begin{aligned}
&\text{For perturbations} \rightarrow \\
&\bar{E}_0 \Leftrightarrow V_0 \\
&\Delta\bar{E} \Leftrightarrow V_1 \\
&\Delta\bar{E} = \bar{E}_0 * \int dt (J_{Josephson} / J_0)^2 \\
&\Delta\bar{E} = \bar{E}_0 \frac{1}{t_0}\int_0^{t_0} dt[\frac{\sin\tilde{T}t \pm 2\cos(2\tilde{T}t - eVt)(1-\frac{eV}{\tilde{T}})\sin(\tilde{T}t - eVt)}{\cos\tilde{T}t \pm 2\cos(2\tilde{T}t - eVt)\cos(\tilde{T}t - eVt)}]^2 \\
&= \bar{E}_0\{\frac{\tan\tilde{T}t_0}{\tilde{T}t_0} - 1\} \text{ for V=0}
\end{aligned} \quad , (21)$$

where

$$\hbar\tilde{T} = eV - V_1$$
$$V : voltage$$

Here $\bar{E}_0$ is the unperturbed energy and $\Delta\bar{E}$ is the energy change in the presence of perturbation.

In the presence of resonance [18] as shown in Figure 3 and Table 1, transfer interactions become $\hbar\tilde{T} \Rightarrow \sqrt{(\hbar\tilde{T} - \hbar\omega_0)^2 + (\hbar\tilde{T}_0)^2}$ ,

where $\tilde{T}_0$ is a constant. At lower temperatures, the band gap [19] plays the role of a superconducting gap:

$$\begin{aligned}
&\text{Imaginary part}\{2\tanh(..) - 1\} \\
&= 2\coth(..) \\
&\frac{1}{N(0)\bar{V}} = \int_0^{\hbar\omega} \frac{2\coth(\frac{\sqrt{\varepsilon^2 + E_R^2}}{2k_BT})}{\sqrt{\varepsilon^2 + E_R^2}} \delta(\varepsilon - \hbar\omega_0) d\varepsilon \\
&\bar{V} = |U_c| \\
&\frac{1}{N(0)\bar{V}} = \hbar\omega \frac{2\coth(\frac{\sqrt{(\hbar\omega_0)^2 + E_R^2}}{2k_BT})}{\sqrt{(\hbar\omega_0)^2 + E_R^2}} \\
&E_R = E_{\text{Resonance}} = E_g = Superconducting\ gap
\end{aligned} \quad , (22)$$

where $\delta$ is a delta function, and $\hbar$ is Planck's constant divided by $2\pi$. The superconducting gap and resonance energy are shown in Figures 4 and 5, where the BCS-type gap is given as

Preprints (www.preprints.org) | NOT PEER-REVIEWED | Posted: 2 January 2024 doi:10.20944/preprints202312.2308.v1



$E_R \equiv \Delta_{BCS} = 52.5(1-(\frac{T}{30})^2)$, the resonance gap is given by $\hbar\omega_0 = 2k_B T_c - 2k_B T$, and the effective or pure BCS-type superconducting temperatures are $T_c = 100\ K, T_c^{BCS} = 30\ K$.

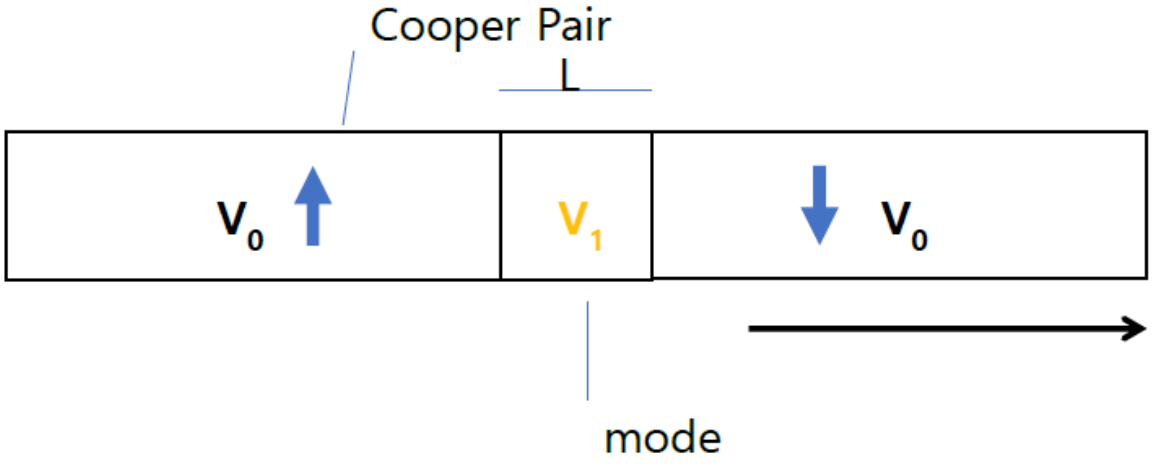


**Figure 3.** Natural resonance termed as Josephson resonance between a Cooper pair is shown where the natural thickness of intercalated insulator in a kind of Josephson junction is given to be the resonance energy, $\hbar\omega_0 = eEL$.

**Table 1.** The criteria may be guessed from that in resistivities temperature linear dependences are subject to CDW and flat dependences are subject to magnons.

| Materials | Resonance with | gain or loss |
|---|---|---|
| HTSC | Amplitudon of CDW | loss |
| HFS | Phason of magnon | gain |
| Graphene | Phason of phonon | gain |
| He3, He4 | Phason of phonon | gain |
| Organic SC | Phason of CDW | gain or loss |
| Nickelate | Phason of CDW | gain or loss |
| Topological SC | Topological order | gain or loss |
| Ru SC | Phason of Magnon | gain or loss |

Preprints (www.preprints.org) | NOT PEER-REVIEWED | Posted: 2 January 2024 doi:10.20944/preprints202312.2308.v1



| | | |
|---|---|---|
| $H_xS_{1-x}$ (pressure-induced) | Amplitudon of Magnon | gain or loss |
| Cobalt Oxide SC | Phason of CDW | gain or loss |

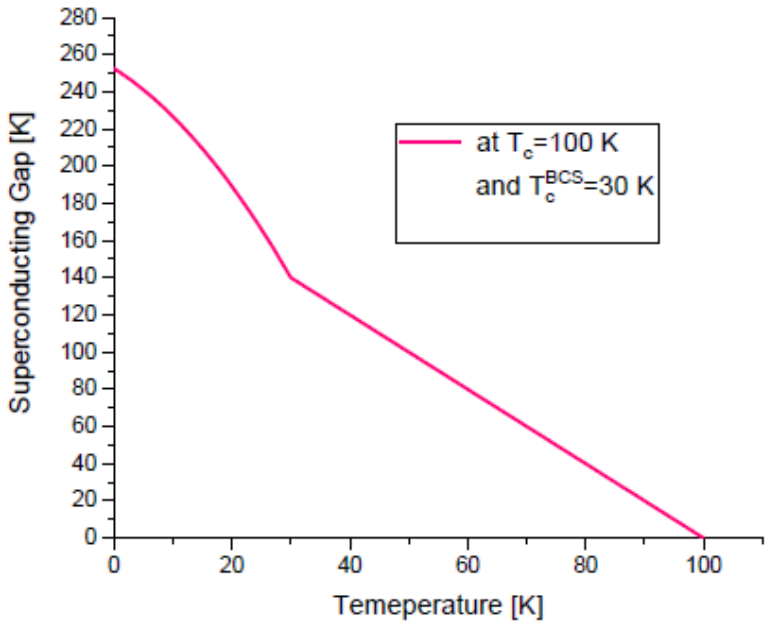


(a)

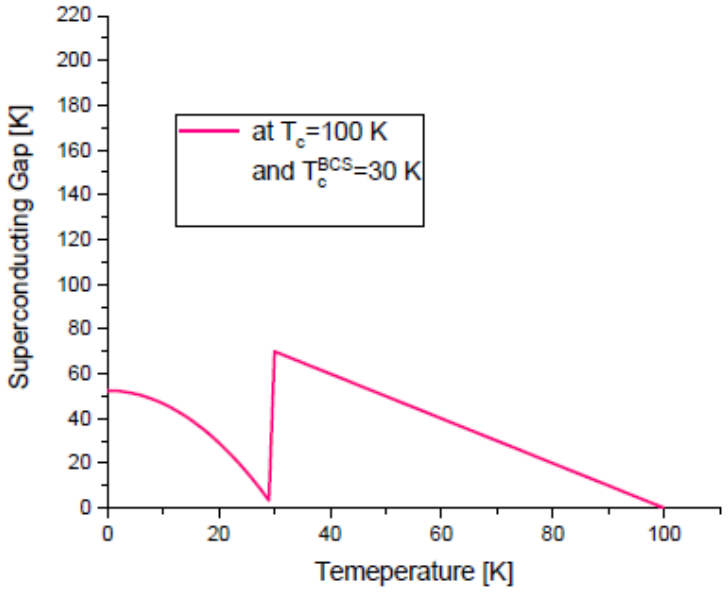


(b)

Preprints (www.preprints.org) | NOT PEER-REVIEWED | Posted: 2 January 2024 doi:10.20944/preprints202312.2308.v1



**Figure 4.** The superconducting gap is shown where in the presence of Coulomb repulsions it is given by (a) and in the absence of those below 30 K it is also given as (b).

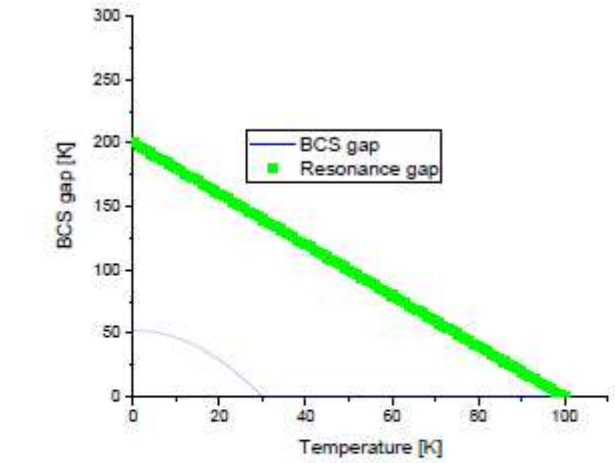


(a)

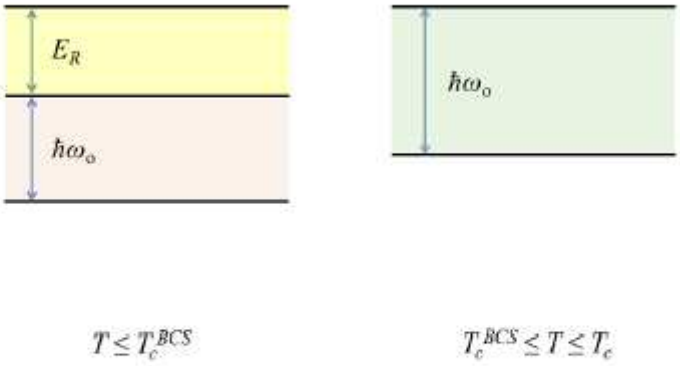


(b)

**Figure 5.** Calculated (a) and illustrated (b) superconducting gap structures.

There is a two-track mechanism when this process occurs in an HTSC. This mechanism includes a superconducting part with a Kwangwoon distribution and a CDW part. Between these resonances inside materials, there is a magnitude of ~100 K, and the effective superconducting temperature will increase from ~10 K to ~100 K as the effective temperature is equal to the superconducting temperature plus the resonance energy. Since CDW is pinned [20], a pinned CDW confined in a quantum well transitions from the 1st to the 2nd levels via resonance, as shown in Figure 6.

Preprints (www.preprints.org) | NOT PEER-REVIEWED | Posted: 2 January 2024 doi:10.20944/preprints202312.2308.v1



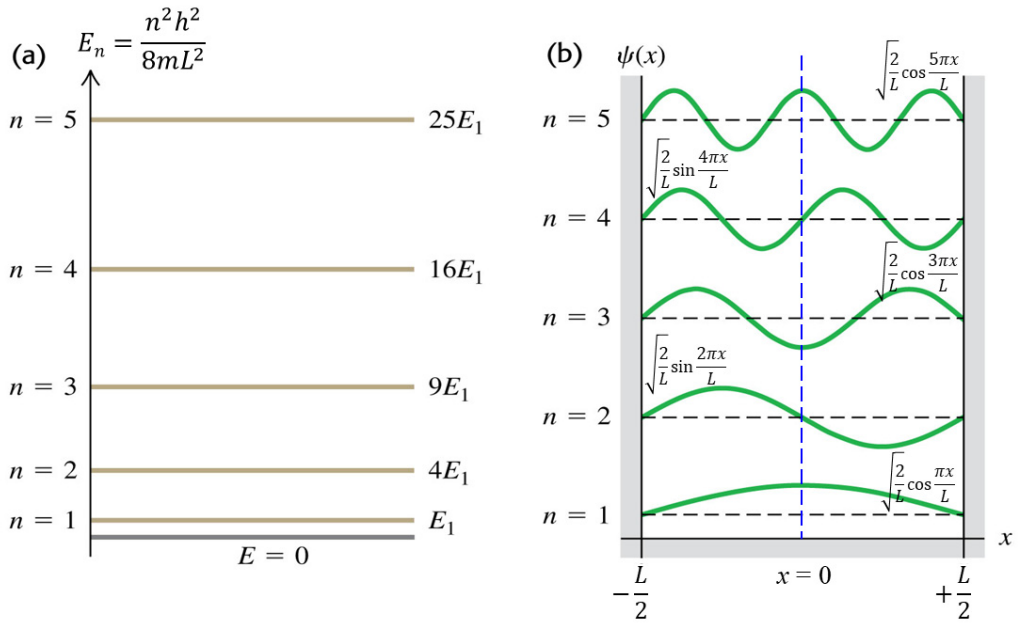


**Figure 6.** CDWs confined as (a) energy levels and (b) wavefunctions.

Let us consider the lifetime of resonances in Eq. (22). The lifetime for single electrons is nearly zero (that is, $\delta(t) \Rightarrow \tau \sim 0$ ), but that for clusters can become infinite (i.e., $\theta(t_0 - |\alpha| \le t \le t_0 + |\alpha|) = \int \delta(t)dt \Rightarrow \tau \sim \infty$ ). We estimate that the 1st level of the quantum well is:

$$\frac{h^2}{8mL^2}|_{L=nm} \sim (10-0.1)eV, \frac{h^2}{8mL^2}|_{L=10nm} \sim (0.1-0.001)eV \quad (23)$$

where $\frac{n^2h^2}{8mL^2} = E_n$, $n = 1,2,3,\ldots$ $m$ , is the mass of an electron participating in a CDW, and $L$ is the size of a pinned CDW. A clue of this resonance mechanism in HTSC is based on the work by Inosov et al. [21], who assigned the spin resonance to some collective mode.

We next consider the magnetic field dependence in normal metallic states [22]. From previous work [23], the relation between magnetic field $H$ and temperature is given as:

$$\frac{1}{\beta}k_BT^{eff} \equiv \frac{1}{\beta}k_BT \pm \mu_BH \quad (24)$$

where $\beta$ is a constant, $\mu_B$ is the Bohr magneton, and the diagonal and off-diagonal conductivity are:

$$\sigma_{xx} = \frac{\partial J}{\partial(\frac{V}{d} = E)}, \sigma_{xy} = \frac{\partial H}{\partial E}\frac{\partial J}{\partial H}$$

$$\sigma_{xx} \propto \frac{1}{k_BT}[\tanh^2(\frac{eV - eV_T}{k_BT}) + 1] \quad (25)$$

$$J \propto [J_0 * H \pm J_1 * k_BT * H]$$

$$eV_T : \text{threshold constant value}$$

where $J_0$ and $J_1$ are constants.

Let us consider the superconducting condensations.

Preprints (www.preprints.org) | NOT PEER-REVIEWED | Posted: 2 January 2024 doi:10.20944/preprints202312.2308.v1



The relation between BCS condensation and Bose-Einstein condensation has been long-standing controversial. Here we suggest a counterproposal as capacitive condensation.

We call a resistance (R) and a capacitance (C) and a voltage (V) in a circuit as RC.

Under the postulation that a Cooper pair have (R,-R), two RC circuits happen as (R, $C_1$,V), (-R, -$C_2$,-V) and capacitive condensation may occur. The negative resistance for a Cooper pair will be discussed in a later work. In brief, in the process of phonon-mediated interactions between the ion and two electrons, the positive resistance is from same amount of energy loss but the negative resistance may stem from the same amount of energy gain. Let us estimate the negative resistance roughly.

For a Cooper pair, it is given as

$$\begin{aligned} \hbar k \to E \to \rho = 1/\sigma = 1/[\frac{\partial \tilde{J}}{\partial E}] \\ -\hbar k \to -E \to -\rho = -1/\sigma = 1/[\frac{\partial \tilde{J}}{\partial (-E)}] \end{aligned} \tag{26}$$

and a negative resistance must be induced to conserve zero total momentum.

Finally, under the postulation of zero Coulomb repulsion at pure BCS-type superconducting states, superconducting gap is modified as

Preprints (www.preprints.org) | NOT PEER-REVIEWED | Posted: 2 January 2024 doi:10.20944/preprints202312.2308.v1



$$i) T \le T_c^{BCS}$$

$$1/(N(0)V) = \int_0^{\hbar\omega} \frac{(2\tanh(\frac{\sqrt{\varepsilon^2+\Delta^2}}{2k_BT})-1)}{\sqrt{\varepsilon^2+\Delta^2}} d\varepsilon$$

$$V = |U_{BCS}|$$

$$k_B T_c^{eff} = k_B T_c^{BCS} + \hbar\omega_0$$

$T_c^{eff}$ : Effective superconducting temperature

$T_c^{BCS}$ : pure BCS superconductng temperature

$\hbar\omega_0$ : resonance energy

$\Delta$ : BCS-type superconducting gap

$U_{BCS}$ : BCS-type electron-electron interaction

N(0):Density of states at Fermi energy

$\hbar\omega$:Debye cut-off energy

$$ii) T_c^{BCS} \le T \le T_c^{eff}$$

imaginary part$\{2\tanh(..)\text{-}1\} \rightarrow 2\coth(..)$

$$1/(N(0)\bar{V}) = \int_0^{\hbar\omega} \frac{2\coth(\frac{\sqrt{\Delta_R^2+\varepsilon^2}}{2k_BT})}{\sqrt{\Delta_R^2+\varepsilon^2}} \delta(\varepsilon-\hbar\omega_0) d\varepsilon$$

$$= \hbar\omega \frac{2\coth(\frac{\sqrt{\Delta_R^2+(\hbar\omega_0)^2}}{2k_BT})}{\sqrt{\Delta_R^2+(\hbar\omega_0)^2}}$$

$$V = |U_c|$$

$\Delta_R \approx k_B T_c^{eff} - k_B T$ : resonance gap

$\Delta^{total} = \Delta + \Delta_R$ : total gap

$U_c$ : Coulomb repulsion (27)

Let us consider the experimental clues for our models.

The simplified dome between transition temperature and hole concentration in high transition temperature superconductors (HTSC) [24] may be approximately fitted by 4th-order function of hole concentration as shown in Figure 7.

Preprints (www.preprints.org) | NOT PEER-REVIEWED | Posted: 2 January 2024 doi:10.20944/preprints202312.2308.v1



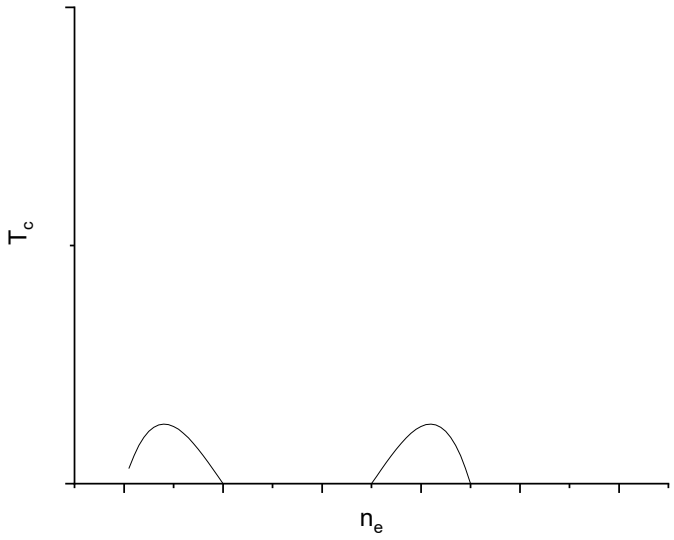


**Figure 7.** Simplified dome between transition temperature and hole concentration in high transition temperature superconductors (HTSC) [34] is shown.

Amongst may models explaining HTSC, resonance-enhanced theory [25] by ours is given as

$$
\begin{aligned}
&T_c = T_c^{BCS} + \hbar\omega_{resonance} = T_c^{BCS} + eEL \\
&eEL \Rightarrow e^* EL^* = eLEn_e' n_h' \\
&e \Rightarrow e^* = (n_e' + n_h')e \\
&\frac{1}{L^*} = (\frac{1}{n_e' L} + \frac{1}{n_h' L}) \\
&T_c^{BCS} : \text{pure BCS transition temperature} \\
&E : \text{electric field} \\
&L : \text{smaple size} \\
&n_i' : \text{effective concentration} \\
&\text{for holes and electrons}
\end{aligned}
\tag{28}
$$

To obtain 4th order function, the so called Berry hole [26] as shown in Figure 7 is inevitable to be introduced and

$$
\begin{aligned}
&n_e' = (a_1 + a_2 n_e)(b_1 + b_2 n_h) \\
&n_h' = (a_1' + a_2' n_e)(b_1' + b_2' n_h) \\
&n_h = (c_1 + c_2 n_e) \\
&a_i, a_i', b_i, b_i', c_i : \text{constant} \\
&n_i : \text{hole or electron concentration}
\end{aligned}
\tag{29}
$$

The anomalies in electronic specific heats in HTSCs [27] using Eq. (28) can be explained as

Preprints (www.preprints.org) | NOT PEER-REVIEWED | Posted: 2 January 2024 doi:10.20944/preprints202312.2308.v1



$$eEL \Rightarrow e^* EL\delta(L-L^*) = eLE\delta(L-L^*)n_e{}'n_h{}'$$
$$eEL \Rightarrow \frac{C_{el}}{T} = \frac{1}{T}\frac{d(eEL)}{dT}$$
$$= \delta(p-p^*)\{\alpha_0 + \alpha_1 p + \alpha_2 p^2 + \alpha_3 p^3 + \alpha_4 p^4\}$$
$$\alpha_i : \text{constants} \qquad . (30)$$
$$p : \text{hole doping}$$
$$p^* : \text{specific hole doping}$$
$$\delta : \text{delta function}$$

In heavy fermion superconductors (HFSs) block spins must be included in the distribution [16]. There may be a singlet of two block spins governed by Brillouin distribution in depressed resonance with magnons. Even though He superconductors, conventional belief is based on boson of He but we may elucidate differently BCS Cooper pairs in resonance with phasons of phonons.

Let us consider gap symmetries in the presence of Kwangwoon distributions.

Because of electron-hole configurations like charge density wave (CDW) sytems [25], gap symmetries of HTSC become

$$\Delta_{HTSC} = A\cos 2k_x^F x + B\cos 2k_y^F y$$
$$= \Delta_d[\cos^2 k_x^F x \pm \cos^2 k_y^F y] + \Delta_0$$

(31)

where $k_x^F$ , $k_y^F$ are Fermi wavevectors along x or y-axis, and $\Delta_d, \Delta_0$ are gaps independent of wavevectors. Under consideration into electrons and holes, the resultant gap becomes

ee

(32)

Let us consider isotope exponents in HTSCs as

$$\alpha \equiv \alpha_{BCS} + \alpha_{\text{Resonance}}$$
$$\alpha = \frac{1}{2} \pm \frac{1}{2}\left(\frac{\frac{1}{2}\hbar\omega_0}{k_B T \pm \frac{1}{2}\hbar\omega_0}\right) \ \text{if } \hbar\omega_0 \propto M^{-\frac{1}{2}} \qquad (33)$$
$$\hbar\omega_0 : \text{Resonance energy} \Leftrightarrow 200\ \text{K (Figure 8)}$$

where M is the mass of ion.

Isotope exponents can be explained by our model regardless of 0, negative, positive values as shown in Figure 8. As shown in Figure 9, the relation between the band gap and Coulomb repulsions may be approximated as

$$E_g = \int_0^{\varepsilon_F - E_g} N(0)U_c(\varepsilon)d\varepsilon$$
$$\approx [N(0)\varepsilon_F]U_c \qquad . (34)$$
$$\varepsilon_F : \text{Fermi energy}$$

Preprints (www.preprints.org) | NOT PEER-REVIEWED | Posted: 2 January 2024 doi:10.20944/preprints202312.2308.v1



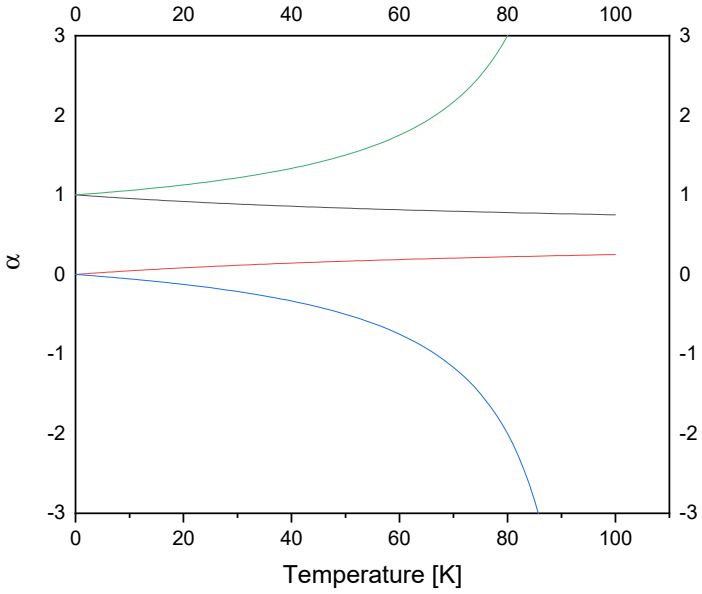


**Figure 8.** Isotope exponents are shown.

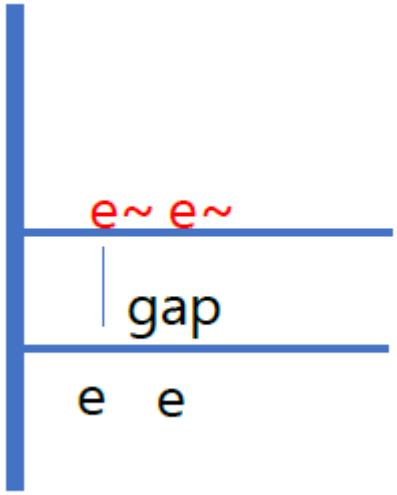


**Figure 9.** The phase diagram is shown where Coulomb repulsion between electrons as e-e , e~-e~ may be zero and non-zero for e-e~ and the band gap stems from Coulomb repulsions.

Using the similar method of Eq. (30) where an electron is equivalent to Berry electron and hole, the superconducting temperature and pseudogap temperature are given by 4th order dependence of hole doping where experimental data [28] for Y-Ba-Cu-O are compared with ours as shown in Figure 10.

Preprints (www.preprints.org) | NOT PEER-REVIEWED | Posted: 2 January 2024 doi:10.20944/preprints202312.2308.v1



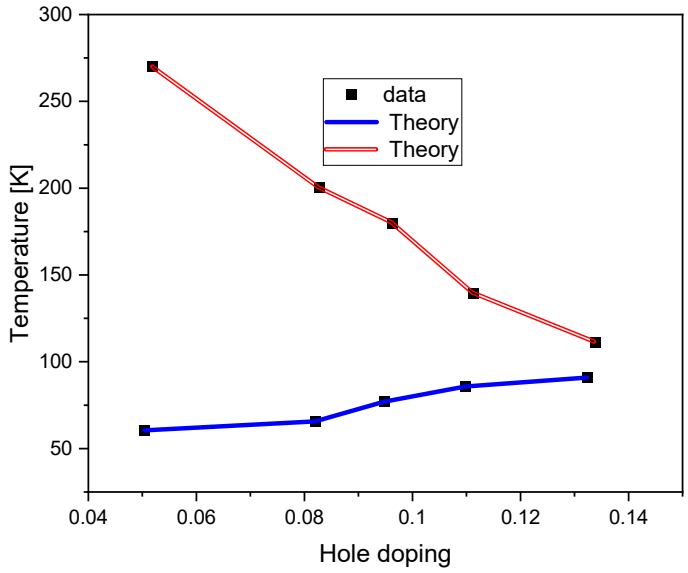


**Figure 10.** The phase diagram is shown where fittings are 562.851-23259.3*x+375012*x^2-2.51539*10^6*x^3+6.09134*10^6*x^4 and 2307.53-94601.6*x+1.58875*10^6*x^2-1.16907*10^7*x^3+3.12701*10^7*x^4.

Let us consider the pressure-induced superconductor [29,30] via resonance using Eq. (22):

$$E_{P_0}: \text{Specific Pressure Energy}$$

$$\frac{1}{N(0)V}=\int_0^{\hbar\omega}\frac{\coth(\frac{\sqrt{\varepsilon^2+E_R^2}}{2k_BT})}{\sqrt{\varepsilon^2+E_R^2}}\delta(\varepsilon-E_{P_0})$$

$$\frac{1}{N(0)V}=\int_0^{\hbar\omega}\frac{\coth(\frac{\sqrt{\varepsilon^2+E_R^2}}{2k_BT})}{\sqrt{\varepsilon^2+E_R^2}}\delta(\varepsilon-E_{P_0})d\varepsilon$$

$$V=|U_{BCS}+U_c|$$

$$\frac{1}{N(0)V}=\hbar\omega\frac{\coth(\frac{\sqrt{(E_{P_0})^2+E_R^2}}{2k_BT})}{\sqrt{(E_{P_0})^2+E_R^2}}$$

$$\text{Though } BCS\Rightarrow T_{SC}\sim 4K$$

$$\hbar\omega_{res}\sim 200K: \text{resonance peak}$$

$$T_{SC}^{eff}\sim(4+200)K \qquad (35)$$

$$E_R=E_{\text{Resonance}}=E_g=\text{Superconducting Gap}$$

The specific heats of He [31] are given as shown below:

$$C_{ph}=\gamma_{ph}T^3$$
$$C_{el}=\gamma_{el}T \qquad (36)$$

in which phononic and electronic ones are described. When phonons undergo freezing, the equation changes:

Preprints (www.preprints.org) | NOT PEER-REVIEWED | Posted: 2 January 2024 doi:10.20944/preprints202312.2308.v1



$$U = N_{ph}(\omega_D)\int_0^{\omega_D} d\omega \frac{\hbar\omega}{\exp(\frac{\hbar\omega}{k_B T})-1}$$

$$= N_{ph}(\omega_D)\alpha T^2$$

$$C_{phonon-freezing} = \frac{dU}{dT} = 2N_{ph}(\omega_D)\alpha T$$

$$\alpha = \frac{k_B^2}{\hbar}(\frac{\pi^2}{6} - ..) \Rightarrow$$

In the case of freezing,

$$\frac{1}{2}\hbar\omega : \text{zero point} \geq k_B T \Rightarrow$$

$$\alpha = \frac{k_B^2}{\hbar}\int_2^{\infty} \frac{x}{\exp(x)-1} dx = \frac{k_B^2}{\hbar}(4 - 3.71 + ...)$$

$$N_{ph}(\omega_D) = \frac{3V\omega_D^2}{2\pi^2 v^3}$$

$$\frac{\pi^2}{6} - .. = 1.6348$$

$$4 - 3.71 + ... = 0.4311$$

$$V : volume$$

$$v : sound\ velocity \qquad (37)$$

$$\omega_D : Debye\ cut - off$$

in which a Fermi level at which electrons are concentrated exists, and zero-point modes of phonons are assumed to be condensed at a specific level.

Based on our previous work [32], the phase of the spin glass may be considered a paramagnetic ordering between block spins comprised by many random spins with most spins aimed in one specific direction. Assuming that all states are possible and that the state is governed by the Fermi–Dirac distributions in a block spin in helium in the presence of magnetic fields along the z-axis, the mean value of the spin operator is given as shown below:

Preprints (www.preprints.org) | NOT PEER-REVIEWED | Posted: 2 January 2024 doi:10.20944/preprints202312.2308.v1



$$
\begin{aligned}
&< S_z > \\
&= \frac{\int_{-\beta g\mu_B SH}^{\beta g\mu_B SH} \frac{S_z}{1+\exp(-\beta g\mu_B S_z H)} d(\beta g\mu_B S_z H)}{\int_{-\beta g\mu_B SH}^{\beta g\mu_B SH} \frac{1}{1+\exp(-\beta g\mu_B S_z H)} d(\beta g\mu_B S_z H)} \\
&= \frac{1}{\beta g\mu_B} \frac{\partial}{\partial H} [\ln \int_{-\beta g\mu_B SH}^{\beta g\mu_B SH} \frac{1}{1+\exp(-\beta g\mu_B S_z H)} d(\beta g\mu_B S_z H)], \\
&\therefore < S_z >= S \tanh[\frac{1}{2} \frac{g\mu_B SH}{k_B T}] \qquad (38) \\
&\therefore < \boxed{S_z} >= \frac{1}{2} \tanh[\frac{1}{4} \frac{g\mu_B H}{k_B T}] \\
&\tanh[\frac{1}{4} \frac{g\mu_B H_{\text{internal}}}{k_B T}] \sim 1 \; at \; T \to 0 \\
&\sim \frac{1}{4} \frac{g\mu_B H_{\text{internal}}}{k_B T} \; at \; T \to \infty
\end{aligned}
$$

in which $H_{\text{internal}}$ can be easily exchanged with other parameters, that is, for pressure, electric field, $g$ is the Lande's factor for a spin, $\mu_B$ is the Bohr magneton, and $S = \frac{1}{2}$ is the magnitude of a spin.

From Equations 36–38, the specific heat for $^3$He [33], in which electrons form a block-like structure, can be explained as shown in equation 39:

$$
\begin{aligned}
&C = \gamma_{el} T \tanh \frac{\tilde{\beta}}{T} + \gamma_{phonon-freezing} T \Rightarrow \\
&at \; T \geq T_c, \Rightarrow \gamma_{el} \tilde{\beta} + \gamma_{phonon-freezing} T \qquad (39) \\
&at \; T \leq T_c, \Rightarrow \gamma_{el} T + \gamma_{phonon-freezing} T \\
&\gamma_{el} T_c - \gamma_{el} \tilde{\beta} \Leftrightarrow Jump \; at \; T_c
\end{aligned}
$$

in which $\tilde{\beta}$ is a constant, and phonon-freezing is postulated. From the experiment of specific heat for $^3$He [34], the parameters are obtained and shown below:

$$
\begin{aligned}
&\gamma_{el} = 0.0407 \times 10^3 \; NR/K \\
&\gamma_{phonon-freezing} = 0.00504 \times 10^3 \; NR/K \\
&\tilde{\beta} = 2.0156 \; \text{mK} \\
&T_c = 2.5888 \; \text{mK:superconducting temperature}
\end{aligned}
\qquad , (40)
$$

where this is in fitting as shown in Figure 11.

Preprints (www.preprints.org) | NOT PEER-REVIEWED | Posted: 2 January 2024 doi:10.20944/preprints202312.2308.v1



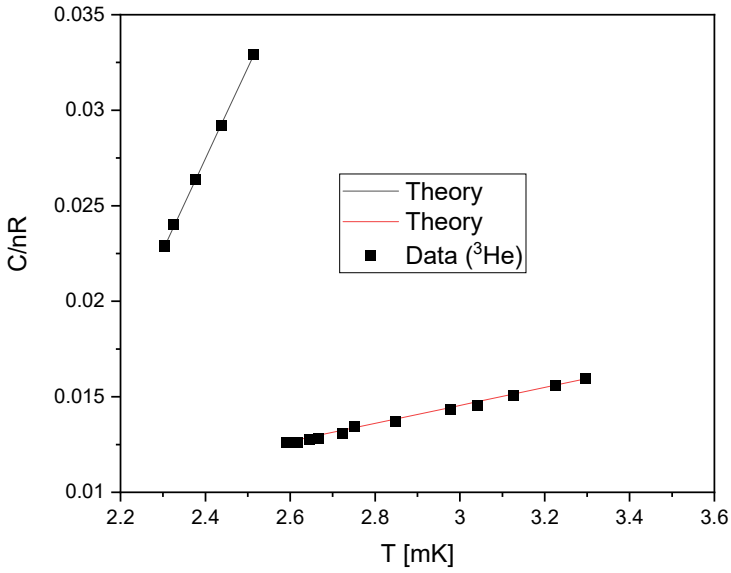


**Figure 11.** Heat capacity of $^3$He is shown.

In the case of $^4$He [34], it was assumed that no phonon freezing occurred, and $T^3$ phonon specific heat is dominant. From the point of view of block spins at specific temperatures, block spins in He I states may be dominant above a specific temperature, however, below this temperature, single spins in He II phases are in the majority. This behavior can be represented in Equation (38) in which the specific heat is given as shown below:

$$C_V = \frac{\partial}{\partial T}[g\mu_B SH \tanh\{\frac{g\mu_B SH}{2k_B T}\}]$$

$$\Rightarrow C_1 - \frac{(g\mu_B SH)^2}{2k_B T^2}[1-\tanh^2\{\frac{g\mu_B SH}{2k_B T}\}] \quad (41)$$

$C_0$ : constant from the pseudo latent heat

$C_1$ : constant from other mechanisms

The total specific heat is given as shown below:

$$C_V^{He\,I} = C_1 - \frac{(g\mu_B SH)^2}{2k_B T^2}[1-\tanh^2\{\frac{g\mu_B SH}{2k_B T}\}] \; at \; T \geq T_0$$

$$C_V^{He\,II} = \gamma_{ph} T^3 \; at \; T \leq T_0 \quad (42)$$

$$C_0 = C_V^{He\,II}(T_0) - C_V^{He\,I}(T_0)$$

From Equation (42), this process in He behaves as a lambda-transition as shown in Figure 12 based on [35].

Preprints (www.preprints.org) | NOT PEER-REVIEWED | Posted: 2 January 2024 doi:10.20944/preprints202312.2308.v1



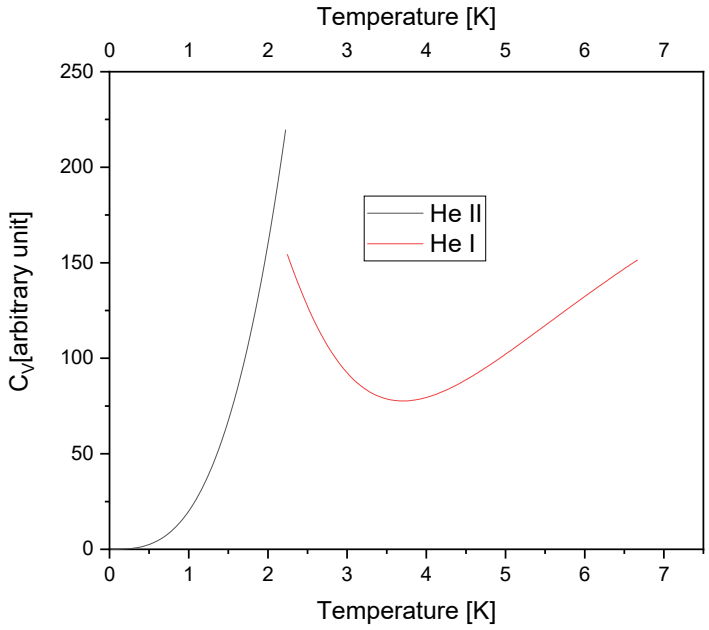


**Figure 12.** An arbitrary lambda-transition is roughly shown.

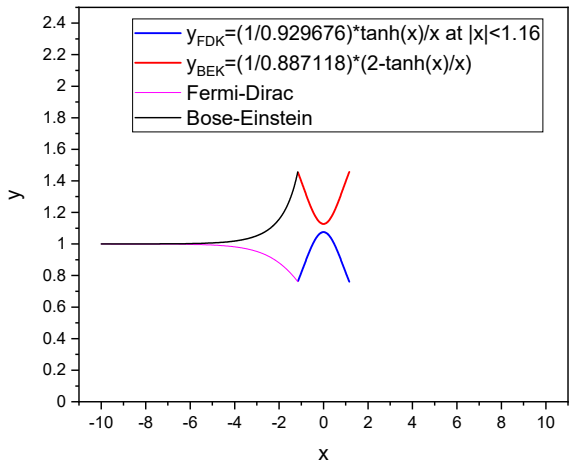


**Figure 13.** New distributions are shown for $|x=\frac{\varepsilon-\mu}{k_BT}|\leq 1.16$ in which the original BE and FD distributions are dominant for $x\leq -1.16$.

It can be assumed that the pseudo latent heat may originate from a difference between higher and lower temperature limits (in fact no latent heat has been observed) as described in Equation 43:

$$\begin{aligned}&\tanh(x\approx 0)\approx x,\\&\tanh(x>>1)\approx 1\\&C_0=\frac{(g\mu_B SH)^2}{2k_BT_0^2}[1-\{\frac{g\mu_B SH}{2k_BT_0}\}^2]-\frac{(g\mu_B SH)^2}{2k_BT_0^2}[1-1]\end{aligned}\qquad(43)$$

The other constant term may originate from Coulomb repulsions of block spins (electrons) from Eq. (38) as

Preprints (www.preprints.org) | NOT PEER-REVIEWED | Posted: 2 January 2024 doi:10.20944/preprints202312.2308.v1



$$C_1 \propto \gamma_{el} T S_{block} \propto \gamma_{el} T \frac{1}{T} \quad \text{at } (T \approx \infty) \quad (44)$$

From Equation (38), Equation (45) can be derived as shown below:

$$< S_z >$$

$$= \frac{\int_{-\beta g \mu_B SH}^{\beta g \mu_B SH} \frac{S_z}{1+\exp(-\beta g \mu_B S_z H)} d(\beta g \mu_B S_z H)}{\int_{-\beta g \mu_B SH}^{\beta g \mu_B SH} \frac{1}{1+\exp(-\beta g \mu_B S_z H)} d(\beta g \mu_B S_z H)}$$

$$= \frac{1}{\beta g \mu_B} \frac{\partial}{\partial H} [\ln \int_{-\beta g \mu_B SH}^{\beta g \mu_B SH} \frac{1}{1+\exp(-\beta g \mu_B S_z H)} d(\beta g \mu_B S_z H)],$$

$$\therefore < S_z >= S \tanh[\frac{1}{2} \frac{g \mu_B SH}{k_B T}]$$

$$C_1 = \frac{\partial}{\partial T} [\boxed{g} \mu_B \boxed{S} H \tanh\{\frac{1}{2} \frac{g \mu_B SH}{k_B T}\}] \quad (45)$$

$$\boxed{S} = \Lambda U_{Coulomb} T^2 \propto U_{Coulomb} T^2$$

$\Lambda$ : constant

$U_{Coulomb}$ : Coulomb repulsion

$$C_1 = \Lambda \boxed{g} \mu_B U_{Coulomb} H \{\frac{1}{2} \frac{g \mu_B SH}{k_B}\}]$$

for which a temperature-quadratic dependence of Coulomb repulsions can be assumed and $\boxed{g}$ is the Lande's factor for a block spin.

From the original derivation [31], the specific heat of He can be given as shown below:

Preprints (www.preprints.org) | NOT PEER-REVIEWED | Posted: 2 January 2024 doi:10.20944/preprints202312.2308.v1



$$C_V = \gamma_{el} T$$

$$= \int_0^\infty (\varepsilon - \varepsilon_F) N(\varepsilon) \frac{df_{FD}}{dT} d\varepsilon$$

$$\approx N(0) \int_0^\infty (\varepsilon - \varepsilon_F) \frac{df_{FD}}{dT} d\varepsilon \Rightarrow$$

$$N(0) \int_{\varepsilon_F}^\infty U_{Coulomb} \frac{df_{FD}}{dT} d\varepsilon = N(0) \int_{\varepsilon_F}^\infty U_{Coulomb} k_B T \frac{df_{FD}}{dT} d \frac{\varepsilon}{k_B T} = C_1 \Leftrightarrow \text{constant}$$

$FD$ : Fermi-Dirac distribution

N($\varepsilon$)(N(0)):Density of states (at Fermi level)

$\varepsilon_F$ : *Fermi energy*

$$\int_{-\infty}^\infty dx x^2 \frac{e^x}{(e^x+1)^2} = \frac{\pi^2}{3}$$

$$\int_0^\infty dx x \frac{e^x}{(e^x+1)^2} = 0.693291$$

$$\gamma_{el} = \frac{\pi^2}{3} N(0) k_B^2 \qquad (46)$$

$$C_1 = 0.69 * N(0) k_B U_{Coulomb} = 0.69 * U_{Coulomb} * \gamma_{el} / (\frac{\pi^2}{3} k_B)$$

In some HTSC materials, the resistivity may be dominant and dependent on quadratic temperature [36]. It can be elucidated as

$$\rho_{eff} = \rho \frac{N}{\boxed{N}} \propto T / \{\tanh(\frac{T_0}{T})\}$$

$$\rho \propto T$$

$T_0$ : specific temperature (47)

$N$ : total number of atoms

$\boxed{N}$ : total number of block atoms

Let us reintroduce heavy fermion superconductors [16].

The distribution termed Brillouin is given as

$$f_{anyon} = \frac{1}{2} S B_{\frac{S}{2}} (\frac{\varepsilon}{2 k_B T}) + \frac{1}{2} S$$

$$\frac{S}{2} : spin, B_S : \text{Brillouin function}$$

. (48)

Using the BCS scheme, the energy gap, $\Delta$ from the singlet pairing of block spins with antiparallel spin configuration, $(\frac{1}{2}, -\frac{1}{2})$ may be obtained as

Preprints (www.preprints.org) | NOT PEER-REVIEWED | Posted: 2 January 2024 doi:10.20944/preprints202312.2308.v1



$$1=\tilde{N}N(0)(|U_{BCS}+U_c|)\int_0^{\hbar\omega}\frac{d\varepsilon[B_{\frac{1}{2}}\{\sqrt{\varepsilon^2+(\Delta)^2}/(2k_BT)\}+1-1]}{\sqrt{\varepsilon^2+(\Delta)^2}}$$
$$\approx\tilde{N}N(0)(|U_{BCS}+U_c|)\int_0^{\hbar\omega}\frac{d\varepsilon\{1-\exp[-\frac{\sqrt{\varepsilon^2+(\Delta)^2}}{2k_BT}\frac{1}{\frac{1}{2}}]\}}{\sqrt{\varepsilon^2+(\Delta)^2}} \quad (49)$$

where this singlet block Cooper pair may be in resonance with some mode, i.e.,) magnons.

Here using appropriate values of effective mass and effective charge, $m^*=\tilde{N}m_e>>m_e \quad (m_e:\text{the mass of bare electron})$, $\tilde{N}:\text{number of spins in a standard block}, e^*=\tilde{N}e$, respectively. As shown in Figure 1 in Ref [16], in the presence of electric fields the effective charge of a block spin can be $e^*=e$.

Let us consider the heat capacity in heavy fermion materials such as $CeCu_2Si_2$ and $UBe_{13}$.

The heat capacity is given as

$$C=\frac{dU}{dT}\approx N(0)\varepsilon_F\int_0^{\infty}d\varepsilon\frac{df_{anyon}}{dT} \quad (50)$$

where $U$ is the energy and $\varepsilon_F$ is the Fermi energy and $N(0)$ is the density of states at Fermi level.

The heat capacity is rewritten as

$$C/T=k_B^2N(0)\varepsilon_F\frac{1}{(Sk_BT)^2}[(Sk_BT)^2+\varepsilon_F(Sk_BT)]\ \ if\ T\ is\ lower$$
$$=k_B^2N(0)\varepsilon_F\frac{\frac{S}{2}+1}{3\frac{S}{2}}\log(|\frac{\varepsilon_0}{k_BT}|)\quad if\ T\ is\ higher\ [\because\int_{k_BT}^{\varepsilon_0}\frac{\varepsilon}{k_BT}d\varepsilon] \quad (51)$$

where $\varepsilon_0$ is a specific mean energy and this calculated heat capacity is in good correspondence with experimental data in $CeCu_2Si_2$ and $UBe_{13}$ [16].

Let us consider the native distributions before forming Boltzmann distributions.

For any distribution, $g(\varepsilon)$ and parameter, $A$, the result is given as

$$g(\varepsilon+A)=g(\varepsilon)\pm g(\varepsilon)(\frac{\tan(\tilde{T}t)}{\tilde{T}t}-1)$$
$$\hbar\tilde{T}=\varepsilon(A):\text{energy of } A, \quad (52)$$
$$\text{distributions will be given as}$$
$$g(\varepsilon+A)/g(\varepsilon)$$

in which the limit is restricted as:

$$\frac{\tan(\tilde{T}t=1.16)}{\tilde{T}t=1.16}-1=1\Leftrightarrow\Delta\bar{E}=\bar{E}_0.$$

From Eq. (21), the modified FD and BE distributions as "Fermi-Dirac-Koo distribution", 4th distribution, and "Bose-Einstein-Koo distribution", 5th distribution are given as shown in the following equations:

Preprints (www.preprints.org) | NOT PEER-REVIEWED | Posted: 2 January 2024 doi:10.20944/preprints202312.2308.v1



$$Fermi-Dirac-Koo = 1/0.929676 * \frac{\tan(\tilde{T}t)}{\tilde{T}t}$$

$$= 1/0.929676 * \frac{\tanh(\frac{\varepsilon-\mu}{k_B T})}{\frac{\varepsilon-\mu}{k_B T}}$$

$$Bose-Einstein-Koo = 1/0.887118 * (2 - \frac{\tan(\tilde{T}t)}{\tilde{T}t})$$

$$= 1/0.887118 * (2 - \frac{\tanh(\frac{\varepsilon-\mu}{k_B T})}{\frac{\varepsilon-\mu}{k_B T}})$$

$$\int_{-1.16}^{1.16} \frac{\tanh(x)}{x} dx = 2.0544$$

$$\int_{0}^{1.16} \frac{\tanh(x)}{x^2} dx = 361.538 \qquad (53)$$

in which the constants, ($1/0.929676$ , $1/0.887118$ ) stem from the continuity conditions, and the Matsubara relation [25] is given as:

$$t = i\frac{\tilde{\beta}}{k_B T \pm k_B T_0}$$

$$i = \sqrt{-1}$$

$$\tilde{T}t = i\frac{\varepsilon-\mu}{k_B T} \qquad (54)$$

$$\tilde{\beta} : \text{constant}$$

$$T_0 : \text{Specific Temperature (at some cases, } T_0 = 0)$$

and $\varepsilon$ is the energy, $\mu$ is the chemical potential, and those are shown in Figure 13.

From Eq. (17), phasons and amplitudons are derivied as

$$J = J_0 \tan(\tilde{T}t)$$

$$0 = \delta J = \delta J_0 \tan(\tilde{T}t) + J_0 \delta(\tan(\tilde{T}t))$$

$$(\delta J)^2 \Rightarrow \tan(\tilde{T}t)\delta(\tan(\tilde{T}t)) \Rightarrow \frac{1}{5}(\tan(\tilde{T}t))^5 + \frac{1}{3}(\tan(\tilde{T}t))^3$$

$$\delta(\tan(\tilde{T}t)) \rightarrow \int[\delta(\tan(\tilde{T}t))]^2 = \tan(\tilde{T}t) + \frac{1}{3}\tan^3(\tilde{T}t) \qquad (55)$$

$$\tan(\tilde{T}t) \Rightarrow \frac{\tan(\tilde{T}t)}{\tilde{T}t} - 1$$

$$\delta[\tan(\tilde{T}t)] \Rightarrow \frac{\tan(\tilde{T}t)}{\tilde{T}t} - 1 + \frac{1}{3}\frac{\tan^3(\tilde{T}t)}{\tilde{T}t}$$

Let us consider magnetic free spins and magnetic domain walls in viewpoint of Neel antiferromagnet with two sublattices. Magnetic free spins as itinerant phasons may be governed by a distribution, 6th distribution called as "JJKim distribution",

Preprints (www.preprints.org) | NOT PEER-REVIEWED | Posted: 2 January 2024 doi:10.20944/preprints202312.2308.v1



$$[\frac{\tanh(\frac{\varepsilon-\mu}{k_BT})}{\frac{\varepsilon-\mu}{k_BT}}-1]/[\int_{-1.16}^{1.16}dx\{\frac{\tanh(x)}{x}-1\}] \quad (56)$$

and magnetic domain walls as stationary amplitudons are governed by a distribution, 7th distribution called as "DJKim distribution",

$$[\frac{\tanh(\frac{\varepsilon-\mu}{k_BT})}{\frac{\varepsilon-\mu}{k_BT}}-1-\frac{1}{3}\frac{\tanh^3(\frac{\varepsilon-\mu}{k_BT})}{\frac{\varepsilon-\mu}{k_BT}}]/[\int_{-1.16}^{1.16}dx(\frac{\tanh(x)}{x}-1-\frac{1}{3}\frac{\tanh^3(x)}{x})] \quad . (57)$$

$$\int_{-1.16}^{1.16}dx(\frac{\tanh(x)}{x}-1-\frac{1}{3}\frac{\tanh^3(x)}{x})=2*(-0.225118)$$

and magnetic skyrmions as coupled phason-amplitudons are governed by a distribution, 8th distribution called as "SSLee distribution",

$$[\frac{1}{5}\frac{\tanh^5(\frac{\varepsilon-\mu}{k_BT})}{\frac{\varepsilon-\mu}{k_BT}}+\frac{1}{3}\frac{\tanh^3(\frac{\varepsilon-\mu}{k_BT})}{\frac{\varepsilon-\mu}{k_BT}}]/[\int_{-1.16}^{1.16}dx(\frac{1}{5}\frac{\tanh^5(x)}{x}+\frac{1}{3}\frac{\tanh^3(x)}{x})] \quad (58)$$

$$\int_{-1.16}^{1.16}dx(\frac{1}{5}\frac{\tanh^5(x)}{x}+\frac{1}{3}\frac{\tanh^3(x)}{x})=0.23342$$

The saturation of resistivity in HTSC [37] by block spins from Eqs. (12) and (38) can be explained by

$$\boxed{\rho}=\rho\frac{\boxed{S}}{S}\propto T\tanh(\frac{T_0}{T})\Rightarrow T(\text{at } T\to 0)$$

$$\Rightarrow T_0(\text{at } T\to\infty)$$

$$\rho\propto T \quad (59)$$

$$\boxed{S}\propto\tanh(\frac{T_0}{T})$$

$T_0$ : specific temperature

**4. Conclusion**

In summary, the emergence of high-temperature superconductivity in cuprates and pnictides may be attributed to an alternative carrier distribution—a novel arrangement within the framework of the BCS scheme. It's crucial to distinguish between spin gaps and pseudogaps. Spin gaps may arise from the disparity between the gap at lower temperature limits and another gap at higher temperature limits. On the other hand, pseudogaps represent a type of superconducting gap for electrons, while pure superconducting gaps can be viewed as gaps tailored for holes. The resonance between superconducting electrons following a traditional BCS model and independent charge density waves (CDWs) could propel the attainment of high transition temperature superconductivity. Clues supporting this notion may be found in the magnetic resonance modes observed in cuprates [38]. Nematic orders [39] manifest in high-temperature superconductors (HTSCs) and can be elucidated through electron-hole spin density waves (SDWs), where both electron CDWs and hole CDWs coexist. The absence of a pseudogap in n-type materials [40] is

primarily attributed not to a new distribution of electrons and holes but rather to a Fermi-Dirac distribution of electrons as described in Equation (11).

In the presence or absence of magnetic fields, nematic phases are observed [41] in HTSC and can be explained as the resonance between ions and the ionic part of a CDW with spacing, 2a (on the contrary, SDW with spacing, 4a, (a:lattice constant)) because CDWs are electron-ion coupled modes. As an analogy, the patterns in HTSC could be considered as rising through resonance liked the striped patterns of rising when bread is baked. From the stripe patterns [42–44], electron-hole CDW (e-h CDW) and e-h SDW may have spacings, 4a, 8a. Fermi arcs [45,46] may be assigned to hole Fermi surface (FS) subtracting from electron FS into remnant arcs. In some HTSC materials within specific doping ranges, CDWs were not observed but these can be solved by the existence of block-CDWs where these are comprised by block spins. I may guess block-CDW and pair density wave and charge density fluctuation are categorized as the same kind [47].

**Acknowledgments:** This work has been funded by a research grant from Kwangwoon University (2023).

## References

1. J.R. Schrieffer, Theory of Superconductivity, Benjamin, New York, 1964.
2. J. Bardeen, L.N. Cooper, J.R. Schrieffer, Phys. Rev. 108 (1957) 1175.
3. J.G. Bednorz, K.A. Müller, Z. Phys. B - Condensed Matter 64 (1986) 189.
4. R.J. Birgeneau, M.A. Kastner, A. Aharony, Z. Phys. B - Condensed Matter 71 (1988) 57.
5. A. Aharony, R.J. Birgeneau, A. Coniglio, M.A. Kastner, H.E. Stanley, Phys. Rev. Lett. 60 (1988) 1330.
6. V. Hizhnyakov, E. Sigmund, Physica C 156 (1988) 655.
7. G. Seibold, E. Sigmund, V. Hizhnyakov, Phys. Rev. B 48 (1993) 7537.
8. P. Monthoux, D. Pines, Phys. Rev. B 47 (1993) 6069.
9. P. Monthoux, J. Phys. Chem. Solids 54 (1993) 1093.
10. P. Monthoux, D. Pines, Phys. Rev. B 49 (1994) 4261.
11. P.W. Anderson, Science 235 (1987) 1196.
12. G. Baskaran, Z. Zou, P.W. Anderson, Solid State Commun. 63 (1987) 973.
13. B.L. Altshuler, L.B.Ioffe, Solid State Commun. 82 (1992) 253.
14. J.R. de Sousa, J.T.M. Pacobahyba, M. Singh, Solid State Commun. 149 (2009) 131.
15. J. Bauer, A.C. Hewson, N. Dupuis, Phys. Rev. B 79 (2009) 214518.
16. J.H. Koo, Y. Kim, J. Supercond. Novel Magn. 29 (2016) 9.
17. J.B. Ketterson, S.N Song, Superconductivity, pp. 326-327, (Cambridge University Press, New York, 1999).
18. J.W. Jewett, R.A. Serway, Physics for Scientists and Engineers with Modern Physics, 8th ed., (Brooks Cole, Singapore, 2010).
19. J.H. Koo, K.-S. Lee, J. Korean Phys. Soc., 76 (2020) 834.
20. J.H. Koo, J.Y. Jeong, G. Cho, Solid State Commun. 149 (2009) 142.
21. D.S. Inosov, et al., Nat. Phys. 6 (2010) 178.
22. N. Singh, Physica C 580 (2021) 1353782.
23. J.H. Koo, M.K. Lee, J.H. Kim, D.J. Jin, G. Cho, Solid State Commun. 164 (2013) 47.
24. E. Fradkin, et al., Rev. Mod. Phys. 87 (2015) 457.
25. J.H. Koo, Eur. Phys. J. Plus 136 (2021) 1020.
26. Y. Kim, J.H. Koo, unpublished (2023).
27. B. Michon, et al., Nature 567 (2019) 218.
28. E. Uykur, et al., Phys. Rev. Lett. 112 (2014) 127003.
29. L.P. Gor'kov, V.Z. Kresin, Rev. Mod. Phys. 90 (2018) 011001.
30. I. Nekrasov, S. Ovchinnikov, J. Supercond. Novel Magn. 35 (2022) 959.
31. C. Kittel, Introduction to Solid State Physics, 5th edition, (John Wiley & Sons, New York, 1976)
32. J.H. Koo, Physica B 457 (2015) 54.
33. J.C. Wheatley, Rev. Mod. Phys. 47 (1975) 415.
34. X. Lin, Ph.D. Thesis, (Penn. State University,2008)(unpublished).
35. R.J. Donnelly, Physics Today, 30-36, July (1995).
36. T. Sarkar, et al., Phys. Rev. B 98 (2018) 224503.
37. D. Bhoi, et al., Supercond. Sci. Technol. 21 (2008) 125021.

 doi:10.20944/preprints202312.2308.v1



38. Y. Sidis, et al., Phys. Stat. Sol. (b) 241 (2004) 1204.
39. A. Chubukov, P.J. Hirschfeld, Physics Today, June (2015) 46.
40. R.L. Greene, et al., Annual Rev. Condens. Matter Phys. 11 (2020) 213.
41. J.A.W. Straquadine, et al., Phys. Rev. B 100 (2019) 125147.
42. J.M. Tranquada, Adv. in Phys. 69 (2020) 437.
43. N.K. Gupta, et al., Phys. Rev. B 108 (2023) L121113.
44. K. Willa, et al., Phys. Rev. B 108 (2023) 054504.
45. X.-C. Wang, Y. Qi, Phys. Rev. B 107 (2023) 224502.
46. F. Restrepo, et al., Phys. Rev. B 107 (2023) 174519.
47. R. Arpaia, G. Ghiringhelli, J. Phys. Soc. Jpn. 90 (2021) 111005.